

A. JULLIEN^{1,2}
S. KOURTEV³
O. ALBERT¹
G. CHÉRIAUX¹
J. ETCHEPARE¹
N. MINKOVSKI³
S.M. SALTIEL³, 

Highly efficient temporal cleaner for femtosecond pulses based on cross-polarized wave generation in a dual crystal scheme

¹ Laboratoire d'Optique Appliquée, UMR 7639: Ecole Nationale Supérieure de techniques avancées – Ecole Polytechnique – Centre National de la Recherche Scientifique, 91761 Palaiseau Cedex, France

² Thales Laser, RD 128, Domaine de Corbeville, 91400 Orsay, France

³ Faculty of Physics, University of Sofia, 5 J. Bourchier blvd., 1164 Sofia, Bulgaria

Received: 7 November 2005/Revised version: 15 May 2006
Published online: 29 June 2006 • © Springer-Verlag 2006

ABSTRACT We present an experimental demonstration of a renewed set up, with respect to the one described in [A. Jullien et al, *Opt. Lett.* **30**, 920 (2005)], that enables more reliable and robust performances in the increase of the contrast ratio (CR) of energetic femtosecond pulses. The new approach is based on the use of two successive crystals situated at optimum position that generate cross polarized waves whose individual effect interferes constructively. This arrangement overcomes the limitation of the single crystal schemes for temporal cleaning – the early saturation of the transmission efficiency, previously observed when either using a relatively thick crystal or increasing intensities up to its damage threshold. A theoretical model that predicts the output CR is developed for the first time. It shows that the CR depends on the initial CR and the extinction ratio of the polarizers used. The measured temporal CR 10^{-10} is in accordance with theoretical predictions.

PACS 42.65.-k; 42.65.Re; 42.65.Jx

1 Introduction

Development of high-peak power laser systems encounters difficulties for the production of pulses with a high temporal contrast (better than 10^{-9}). A typical 100 TW Ti:Al₂O₃ laser configuration, based on a chirped pulse amplification (CPA) scheme, produces femtosecond pulses with short prepulses and postpulses and an amplified spontaneous emission (ASE) nanosecond pedestal. This background is mostly generated in the preamplifier (multipass or regenerative amplifier) and then amplified in power amplifiers, whereas parasitic pulses result from the use of polarizing elements or active correction of spectral characteristics. Consequently, the temporal contrast ratio (CR) of such lasers usually reaches six or seven orders of magnitude. This value of CR is a limitation for high-field physic experiments, when the laser beam is focused with an intensity of about 10^{21} W cm⁻² on a solid target. This laser pulse has to be free of pedestal or prepulses to avoid production of preplasma before the

main pulse reaches the target [1]. To increase the pulses temporal CR, some new schemes are proposed, such as designing more energetic oscillators (more than 100 nJ) [2, 3] to decrease the gain of the pre-amplifier. Other techniques, implementing a saturable absorber [4], or fast Pockels cells, or plasma mirror [5] in the laser chain are investigated. It has also been demonstrated that a promising way to clean the pulse after preamplification is to use a nonlinear filter for femtosecond pulses. This was illustrated by elliptical polarization rotation in hollow waveguides filled with xenon [6]. As this scheme limited the input energy to about 100 μJ, other setups filtering at the millijoule level have been designed. These filters are based on a nonlinear Sagnac interferometer [7], and nonlinear polarization rotation directly in air [8, 9]. Such cleaners may be included in a double CPA system [10]. We have already reported the use of a nonlinear filter based on cross-polarized wave generation (XPW) in a single cubic crystal [11] with a Ti:Al₂O₃ femtosecond laser system at 800 nm. The same kind of filter was used for experiments with a femtosecond 1.053 μm laser [12]. This kind of filter is achromatic, scalable in energy and robust, as the nonlinear process occurs in a solid medium. An energy transmission of 10% was achieved. We demonstrated that the temporal CR was improved by more than four orders of magnitude, the ASE intensity level was brought down to 10^{-10} and the spatial profile was filtered. For these conversion levels, the cleaned pulse presented no spectral phase distortions. The setup of the filter is simple: the input pulse is linearly polarized and focused; the input energy determines the choice of the focal length. We used BaF₂ crystals, 1 mm or 2 mm long, placed near the focus point to optimize the conversion process by reaching the correct peak intensity level ($\approx 10^{12}$ W cm⁻²). The crystal is rotated at an angle $\beta = 22.5^\circ$ between the input polarization direction and its [100] axis. An analyzer then transmits the XPW generated signal. The nonlinear filter based on XPW generation presents good enough performances to be implemented in future laser systems. For this purpose it is of prime importance to know the limitations of this filter in terms of CR improvement and transmission efficiency.

In this paper, we present both theoretical and experimental investigations of the use of XPW process for femtosec-

 Fax: +359 2 96 25 276, E-mail: saltiel@phys.uni-sofia.bg

ond pulse filtering. A theoretical model predicting the XPW cleaner output contrast ratio is described. Experiments were performed on two different femtosecond lasers (a dye laser: 620 nm, 150 μ J, 100 fs, 10 Hz; a CPA laser: 800 nm, 2 mJ, 47 fs, 1 kHz). Due to the achromaticity of the XPW process, experiments at different wavelengths can be directly compared. The paper is organized as follows: in Sect. 2 we analyze two aspects of the XPW process that limit the filter performances, namely the contrast ratio and transmission efficiency. In Sect. 3 we present a 2-crystal setup that we have designed to drastically improve the performances of a temporal cleaner based on XPW generation in cubic non-linear crystals, in terms of efficiency and reliability.

2 Theoretical aspects for the application of XPW process to temporal cleaning of femtosecond pulses

2.1 Effective efficiency in XPW generation

General equations that govern the coupling between two waves have been extensively studied. Applications to the case of two orthogonally polarized waves have also concerned a lot of publications. In continuity to our previously published works [13, 14], we derive here the connection between the general case of plane wave solution and the practical case of currently used spatial and temporal pulse shapes. This is a necessary step to predict experimental efficiency. We define the experimental efficiency of the XPW conversion process as: $\eta_{\text{exp}} = \frac{S_{\text{out}}}{S_{\text{in}}}$, the ratio between crossed and initial polarization wave signals measured using a detector that integrates in space and time. In the non depleted regime [13], the theoretical efficiency η_{theor} that is defined as the squared ratio between the input field A_0 and its orthogonally polarized component B at the crystal output can be described by a \sin^2 function: $\eta_{\text{theor}} = \left| \frac{B}{A_0} \right|^2 = \left(\frac{\gamma_{\perp}}{\gamma_{\parallel}} \right)^2 \sin^2(\gamma_{\parallel} |A_0|^2 L/2) = \frac{I_{\text{out}}}{I_{\text{in}}}$, where γ_{\parallel} and γ_{\perp} are quantities that depend on the third order susceptibility and its anisotropy for a crystal of length L . This formula demonstrates that the nonlinear phase shift encountered by both waves prevents the coherent growing of the

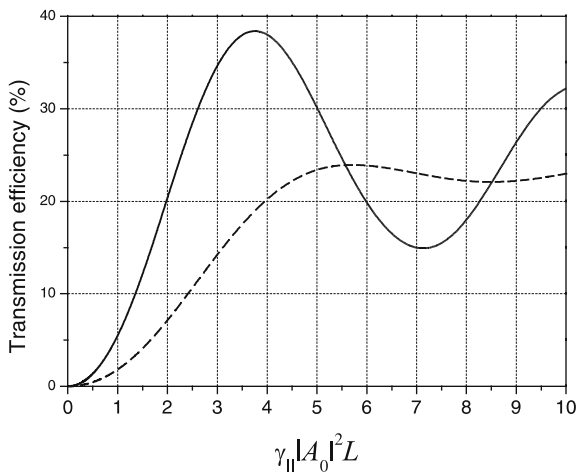


FIGURE 1 Evolution of the conversion efficiency as a function of the spatial and temporal pulse shapes used: rectangular in space and Gaussian in time (solid line); Gaussian in space and Gaussian in time (dashed line)

process of the XPW along the whole length of the sample and introduces the saturation and the periodic character of the efficiency dependence on input intensity.

On going from this plane wave solution (for which η can be ascribed as a peak efficiency η_{peak}) to actual pulses characterized by spatial Gaussian and temporal secant hyperbolic squared shapes, the overall effective efficiency η_{eff} is reduced. As XPW generation is a third order process, the output intensity is proportional to the cube of the input intensity profile in space and time. Therefore, in the non depleted regime, η_{eff} drops down to: $\eta_{\text{eff}} = K\eta$, where the integration constant for these temporal and spatial shapes was obtained as $K = \frac{8}{45}$. This constant K can nevertheless reach a value up to 0.48 when using top-hat spatial profile pulses. This first approximation of XPW efficiency is sufficient for the calculation of the XPW final contrast as will be shown below.

For an accurate comparison with experimental efficiency we have performed numerical calculations for the more general scheme of coupled differential equations that take into account energy transfer between the two beams, cross phase modulation and four wave mixing processes [14]. The β value of the angle between [100] axis of the crystal and the direction of polarization of the input beam (angle that enters in the definition of γ_{\perp}) has been taken as 22.5° . Furthermore, results have been integrated in time and space to simulate two typical laser pulses with a Gaussian temporal profile: a Gaussian or top hat space profile. Figure 1 presents the evolution of the efficiency for Gaussian and top hat pulses of the XPW generation efficiency relative to the (nonlinearity \times intensity \times crystal length, i.e. $\gamma_{\parallel} |A_0|^2 L$) value. The maximum efficiency obtainable in single crystal is about 22% for a Gaussian pulse and 37% for a top hat pulse. These behaviors are a direct consequence of the non-linearity in the conversion process through pulse shape characteristics. It is inducing a reduction of the overall efficiency for a smooth spatial profile like the Gaussian profile compared to the flatter profile like a top hat. As we previously discussed, the reason for the quasi periodic character of the efficiency dependence on input intensity is the nonlinear phase shifts collected by both waves that prevent the coherent growing of the process of the XPW for the whole length of the sample.

2.2 Inherent limitation in the use of an XPW generation process for cleaning fs-pulses

In this paragraph we present an estimation of the output contrast ratio for the pulse temporal cleaner based on XPW generation in crystal(s) sandwiched between the crossed polarizer and analyzer. They are used to isolate the cross polarized wave signal from the input beam. To derive the output CR, let us consider that the input pulse behind the input polarizer is a sum of two contributions. The first one corresponds to the main input femtosecond pulse and has a peak intensity $I_{\text{in,fs}}$. The second one, named the pedestal, is made of contributions going from a ps to a ns time scale and will be noted as $I_{\text{in,pdl}}$. In the same way, we introduce $I_{\text{out,fs}}$ and $I_{\text{out,pdl}}$ to describe the output pulse measured after the analyzer. The input and output contrast ratios are: $C_{\text{in}} = \frac{I_{\text{in,pdl}}}{I_{\text{in,fs}}}$ and $C_{\text{out}} = \frac{I_{\text{out,pdl}}}{I_{\text{out,fs}}}$. We make the hypothesis that the XPW gener-

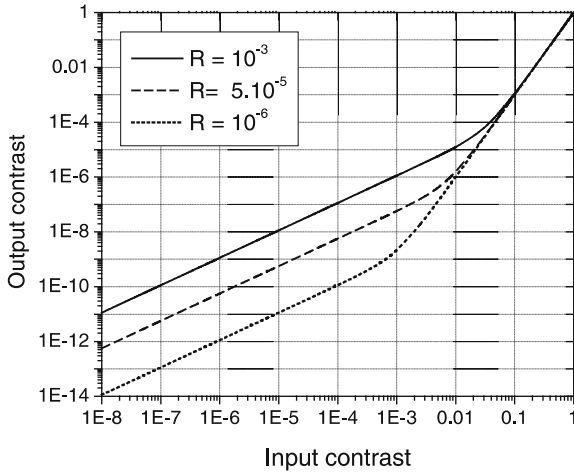


FIGURE 2 Output contrast ratio as a function of input contrast ratio for three different extinction ratios R of the polarizer-analyzer pair

ation process occurs in a non-depleted regime. This assessment does not lead to a loss in generality for the conclusions and allows an easier analytical development. We note η_{fs} and η_{pdl} as being respectively the peak efficiency (plane wave solution) for the main ultra-short pulse and for the pedestal:

$$\eta_{fs} = \frac{I_{XPW,fs}}{I_{in,fs}} = \left(\gamma_{\perp} |A_{0,fs}|^2 L \right)^2, \quad (1)$$

$$\eta_{pdl} = \frac{I_{XPW,pdl}}{I_{in,pdl}} = \left(\gamma_{\perp} |A_{0,pdl}|^2 L \right)^2. \quad (2)$$

The output femtosecond signal is the sum of the femtosecond XPW generated signal and the leakage of the input femtosecond signal from the polarizer analyzer pair. The same observation is valid for the pedestal.

$$I_{out,fs} = I_{XPW,fs} + R I_{in,fs} = \eta_{fs} I_{in,fs} + R I_{in,fs}, \quad (3)$$

$$I_{out,pdl} = I_{XPW,pdl} + R I_{in,pdl} = \eta_{pdl} I_{in,pdl} + R I_{in,pdl}, \quad (4)$$

where R corresponds to the extinction ratio of the used polarizer-analyzer pair. Taking into account the temporal and spatial shape of the pulse, we finally obtain

$$C_{out} = C_{in}^3 \frac{1 + \frac{KR}{C_{in}^2 \eta_{eff}}}{1 + \frac{KR}{\eta_{eff}}}. \quad (5)$$

The output CR depends therefore on three parameters: the overall efficiency $\eta_{eff} = K\eta_{fs}$ of the XPW process, the input pulse contrast and the extinction ratio R of the pair polarizer-analyzer. The overall behavior of the expression (5) is shown on Fig. 2. In Sect. 3.3 we will compare the predictions from (5) and Fig. 2 with the experimentally measured contrast ratio.

3 Experimental results

3.1 Efficiency of the XPW process

Experimental findings for transmission efficiencies that illustrate the considerations from Sect. 2 are drawn in Fig. 3. They concern measurements performed with 1 kHz

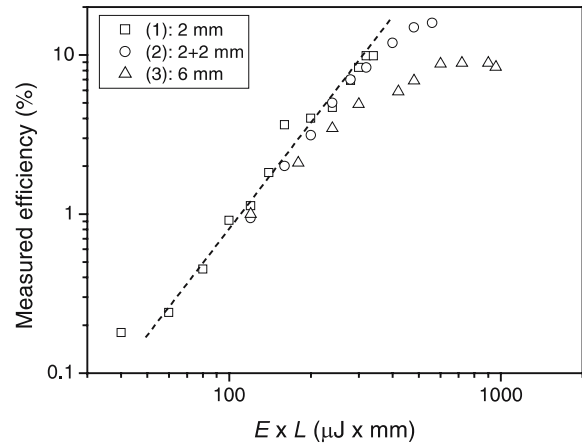


FIGURE 3 Evolution of the experimental efficiency (in %) as a function of the product EL (in $\mu\text{J mm}$) for different crystal lengths. The straight dashed line corresponds to a quadratic law

repetition rate Ti:Al₂O₃ CPA laser. We discuss at this stage curves numbered (1) and (3) that have been obtained using respectively a thin BaF₂ crystal (2 mm long) and a thick BaF₂ crystal (6 mm long). The crystal is not moved during the experiments so the energy is proportional to the intensity on the sample. In case (1), the point that gives rise to the highest efficiency has been obtained using 160 μJ energy pulses, close to the BaF₂ damage threshold for this setup. We verify otherwise the quadratic law over one decade in energy. Case (3) is dramatically different. At equivalent energy-times-length values, the efficiency is lower than for the thin crystal and the quadratic law is no longer observed. Furthermore the efficiency saturation comes close to 10%. We observed in this case, large self-focusing of the beam in the bulk leading to higher intensity and excessive self phase modulation which causes the departure from phase matching. We are therefore outside of the scope described by our model [14]. As a conclusion, we notice the two limitations that prevent us from increasing the XPW efficiency above 10%: (i) using thick crystals leads to unwanted physical processes that tend to compete with XPW generation, and (ii) increasing the intensity results in getting close to the damage threshold for thin crystals that are less sensitive to limitation (i). It has disastrous consequences on crystal degradation and signal instability (spatial hot spots and laser fluctuation).

3.2 Double crystals scheme: XPW interference

To overcome these drawbacks, i.e. reaching and overreaching the theoretical efficiency of a thick crystal, we have developed a new arrangement that consists of the use of several successive thin crystals. We have essentially analyzed a scheme with two BaF₂ crystals. To better clarify the way the double crystals scheme works, we separately investigate the low intensity and high intensity cases.

3.2.1 Low input intensity. For this level of intensity the conversion efficiency is very weak ($\eta_{fs} \ll 1$) and we can neglect the depletion of the fundamental field. Under these conditions, a first crystal generates an XPW field labelled E_{XPW} . In the same way, the fundamental pulse will generate, in a cor-

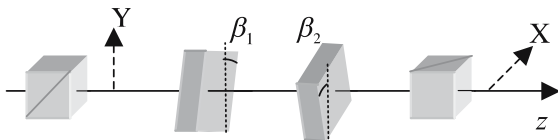


FIGURE 4 Schematic of the dual crystal experiment

rectly oriented second crystal, another field $E'_{XPW} = \alpha E_{XPW}$, where α is the efficiency ratio between the two crystals (for simplicity, we will suppose that the two crystals have the same length). As E_{XPW} and E'_{XPW} result from the same process in the same material, they present the same temporal characteristics. If the two crystals are very close one to each other, the input spatial profile is similar on the two samples, E_{XPW} and E'_{XPW} are then spatially identical and $\alpha = 1$. Consequently the two fields are able to efficiently interfere in the second crystal and the overall efficiency is four times higher. The experimental validation of this process has been achieved using a CPM dye laser. The schematic of the setup is shown in Fig. 4. We introduce β_1 (β_2) the angle of crystallographic [100] axis of the first (second) crystal in the plane perpendicular to the propagation direction with respect to the polarization direction of the input field. We recall that the dependence of XPW amplitude in a single crystal is $F_1(\beta_1) = \sin(4\beta_1)$ [15]. When the two crystals are situated one after the other, the angular intensity dependence will be

$$(F_2(\beta_1, \beta_2))^2 = (\sin(4\beta_1) + \sin(4\beta_2))^2. \quad (6)$$

Now, if one of the crystals is fixed at some of the angles $\pi/8 + m\pi/4$ (the positions of the XPW efficiency maximum), the XPW angular intensity dependence will be finally

$$(F_2(\beta_2))^2 = (1 + \sin(4\beta_2))^2. \quad (7)$$

A two crystal scheme will give, at angles $\beta_2 = \pi/8 + m\pi/2$, four times more XPW signal than a one crystal scheme. The experimental demonstration is given in Fig. 5. There, we show that the rotation of the second crystal allows the suppression of the XPW signal when interference is destructive or increases the efficiency by nearly a factor of four for constructive interference. Solid lines represent theoretical calculations, which are in good agreement with experimental observations. The theoretical model detailed in [14] is used at low input intensity level when $\eta_{fs} \ll 1$ and the Kerr lens effect can be neglected. From the point of view of maximum achievable efficiency at this very low level of input intensity, the schemes with two identical crystals and one double length crystal give exactly the same conversion efficiency.

3.2.2 High input intensity. To illustrate the efficiency of the interfering XPW generated pulse setup at higher intensities, we measured the XPW efficiency for a double crystals scheme with two thin 2 mm long BaF₂ crystals. The experimental device is the same scheme shown in Fig. 4 with a $f = 1$ m focusing lens. Thanks to the two crystals scheme, we were able to greatly improve the XPW efficiency. The 16% efficiency shown in Fig. 3, curve (2) corresponds to 20% internal efficiency. To reach this efficiency value, we searched for the distance between the two crystals which optimized the transmission. In this configuration, the maximum efficiency was

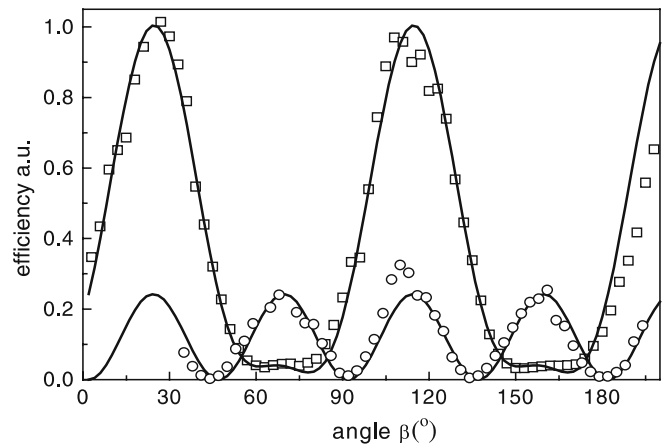


FIGURE 5 Evolution of the efficiency as a function of β angle(s) in a one (circles) and a two (squares) crystal scheme for low intensity excitation. In the two crystal scheme $\beta_1 = 22.5^\circ$

obtained for an optimal distance of 50 mm. We have experimentally demonstrated that the double thin crystals scheme allows reaching of a high XPW efficiency not accessible with a single crystal whatever its length is. This observation is of prime importance for the practical use of the temporal cleaners based on XPW generation.

Compared to the low input intensity regime, the XPW efficiency increase has a totally different explanation. Suppose the input intensity is so high that the XPW generation process in the first crystal is close to the saturation, where the depletion of the fundamental cannot be neglected. In this regime the process efficiency deviates from the quadratic dependence with input intensity. Adding the second crystal with length L_2 with zero separation after the first one with length L_1 will not give $(1 + L_2/L_1)^2$ improvement. It will lead to a very small improvement since saturation has already started (as demonstrated with the use of 6 mm crystal in Fig. 3). As we noted before, the saturation is connected with a non-optimal phase relation between the fundamental wave and the XPW. The reasons for the improved efficiency at certain optimal distance are:

- (i) Kerr lens refocusing of the fundamental beam in the space between the two crystals that leads to a smaller diameter in the plane of the second crystal. Furthermore, Kerr lensing is filtering the fundamental beam from its high spatial frequencies creating a cleaner beam on the second crystal. Therefore XPW efficiency in the second crystal is improved.
- (ii) Achievement of optimal phase shift between the fundamental wave and the XPW at the input of the second crystal. The change of the phase shift between these two waves is due to different accumulation of Gouy phase by propagation in the space between the crystals. The fundamental wave is more intensive, and is more strongly focused by the Kerr lens effect and consequently collects more Gouy phase shift. Recovering the optimal (or close to optimal phase shift) at the input of the second crystal leads to a good phase matching between the generated XPW signals in the two crystals. They are in phase and can interfere constructively.

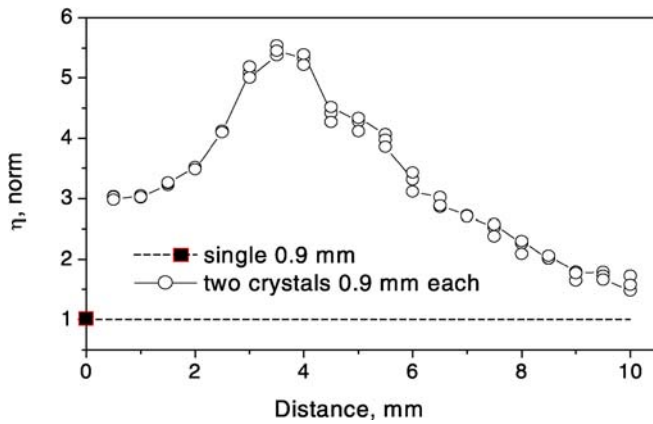


FIGURE 6 Experimental dependence of the XPW conversion efficiency as a function of the two YVO₄ crystals separation. Fundamental radiation with energy of 0.75 μ J is focused with a 30 cm focal length lens. The curve is normalized to the efficiency of the single crystal

(iii) Possibility for independent optimization of the angles β_1 and β_2 .

The influence of these factors depends on the distance between the two crystals that has to be experimentally optimized. To illustrate the role of distance optimization, and to demonstrate another example of the possibility, with two crystals of the same length, to obtain more efficiency than with one crystal twice as long, we present in Fig. 6 an experimental optimization of the two crystals scheme with YVO₄ crystals performed with a 100 fs CPM dye laser. As seen from Fig. 6, for the two crystals at a minimum distance (which is equivalent to a single double length crystal) efficiency is improved by a factor of 3, instead of 4, evidencing the beginning of the saturation regime. On the contrary, at the optimum position, the increase of efficiency of the two crystals scheme is 5.5. This value is significantly higher than the four times improvement expected with a twice thicker crystal in the nondepleted regime. Almost a doubly improved efficiency at an optimum distance with respect to the 0.5 mm distance clearly indicates that phase matching in the second crystal is recovered. This is related to the accumulated Gouy phase on each beam. Furthermore, the efficiency improvement is better than in the case of a long crystal thanks to a cleaner and tighter focusing in the second crystal. This effect also saturates, as the intensity increases. It is limited by the theoretical maximum efficiency that can be reached for a Gaussian pulse in space and time. As it is visible in Fig. 3, curve (2), this saturation is beyond the saturation for a single crystal scheme (1.6 times higher in the case of Fig. 3).

To conclude, we demonstrated that at the low intensity level the two crystals scheme is equivalent to a double length crystal (i.e. increased efficiency by a factor of 4). At high intensities in the regime of pump depletion, the increase of efficiency can be higher than 4 and after that drops with a further increase of intensity.

We have recently reported a more detailed comparison between experimental results and theoretical predictions of the 2-crystal XPW generation schemes under high intensity excitation [16, 17].

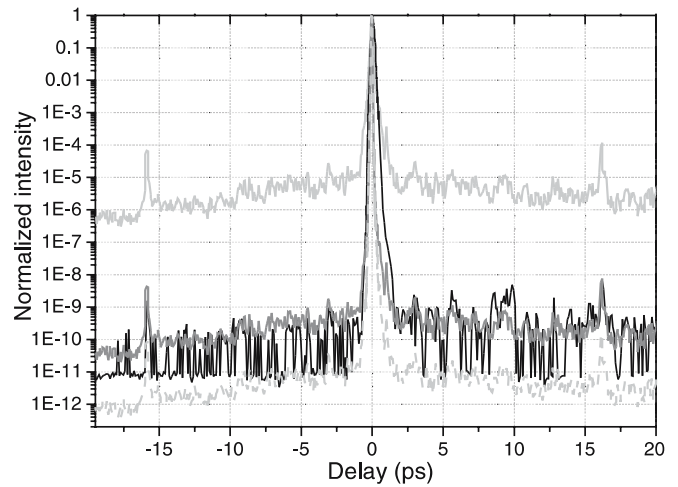


FIGURE 7 Autocorrelation curves measured before (*light gray curve*) and after (*black curve*) filtering with an XPW generating device. The theoretical curves for $\eta_{\text{eff}} = 10\%$ and $R = 5 \times 10^{-5}$ (*gray curve*) and the theoretical curves for $\eta_{\text{eff}} = 10\%$ and $R = 5 \times 10^{-6}$ (*light gray dotted curve*) are shown

3.3 Contrast ratio measurements

Equation (5) have been applied to experimental contrast improvement measurements, where $\eta_{\text{eff}} = 10\%$ and $R = 5 \times 10^{-5}$ [11]. An experimental filter was designed with a 1.2 mJ pulse at 800 nm. Figure 7 shows third-order high dynamical cross-correlation curves before and after filtering. The theoretical curve calculated with the experimental parameters according (5) is also plotted and shows good agreement with the measured temporal profile. The ASE background level value compared to the peak intensity is measured to be reduced by more than four orders of magnitude as the model described in part 2 predicts. We have also plotted the theoretical curve corresponding to $\eta_{\text{eff}} = 10\%$ but with $R = 5 \times 10^{-6}$. This value represents what we would get with better polarizers (10^{-6} is obtainable with current technology). The CR of the output pulse would reach 10^{-12} . It turns out that the major limiting factor seems in fact to be the characteristics of this passive optical element.

4 Conclusion

In this study we focused on the prime limitations of the method of femtosecond pulse cleaning by XPW generation and examined the ways to overcome its drawbacks. Regarding the efficiency of the XPW generation process, we have demonstrated that the two crystals scheme allows working at lower energy levels, which avoids working close to the damage energy threshold of the non-linear crystal. This scheme also enables re-optimising of the phase shifts between the fundamental and XPW wave in the second crystal. This ensures constructive interferences of the signals generated in both crystals and higher overall efficiency. This means reaching a higher transmission for applications like pulse cleaners. The stability of the setup for a day to day utilization and the undamaged life time of the crystals are ensured due to the reduced intensity on each crystal. The model presented here allows prediction of contrast ratios of femtosecond cleaners based on XPW generation. It shows that the most critical element in these types of cleaners is the polarizer-analyzer

pair. The polarizer-analyzer pair has to be chosen with a high extinction ratio, 10^6 or higher if possible, to obtain contrast ratios in the range 10^{-11} – 10^{-12} .

ACKNOWLEDGEMENTS This work has led to a patent application by LOA and Thales Laser [18]. The authors acknowledge the support of the program “Access to Research Infrastructure” contract (LaserLab-Europe, R[3-CT-2003-506350). N.M., S.K. and S.S. thank the Laboratoire d’Optique Appliquée for the hospitality and support during their stay, and also the Bulgarian Ministry of Science and Education for partial support with grant No 1201/2002.

REFERENCES

- 1 K.B. Wharton, J.M. Kim, B.C. Stuart, *J. Appl. Phys.* **97**, 103303 (2005)
- 2 A.M. Kowalevicz Jr., A. Tucay Zare, F.X. Kärtner, J.G. Fujimoto, S. Dewald, U. Morgner, V. Scheuer, G. Angelow, *Opt. Lett.* **28**, 1597 (2003)
- 3 A. Fernandez, T. Fuji, A. Poppe, A. Fürbach, F. Krausz, A. Apolonski, *Opt. Lett.* **29**, 1366 (2004)
- 4 J. Itatani, J. Faure, M. Nantel, G. Mourou, S. Watanabe, *Opt. Commun.* **148**, 70 (1998)
- 5 G. Doumy, F. Quere, O. Gobert, M. Perdrix, P. Martin, P. Audebert, J.C. Gauthier, J.P. Geindre, T. Wittmann, *Phys. Rev. E* **69**, 026402 (2004)
- 6 D. Homoelle, A.L. Gaeta, V. Yanovsky, G. Mourou, *Opt. Lett.* **27**, 1646 (2002)
- 7 A. Renault, F. Augé-Rochereau, T. Planchon, P. d’Oliveira, T. Auguste, G. Chériaux, J.-P. Chambaret, *Opt. Commun.* **248**, 535 (2005)
- 8 A. Jullien, F. Augé-Rochereau, G. Chériaux, J.-P. Chambaret, P. d’Oliveira, T. Auguste, F. Falcoz, *Opt. Lett.* **29**, 2184 (2004)
- 9 M.P. Kalashnikov, E. Risse, H. Schönngel, A. Husakou, J. Herrmann, W. Sandner, *Opt. Express* **12**, 5088 (2004)
- 10 M.P. Kalashnikov, E. Risse, H. Schönngel, W. Sandner, *Opt. Lett.* **30**, 923 (2005)
- 11 A. Jullien, O. Albert, F. Burgy, G. Hamoniaux, J.P. Rousseau, J.-P. Chambaret, F. Augé-Rochereau, G. Chériaux, J. Etchepare, N. Minkovski, S.M. Saitiel, *Opt. Lett.* **30**, 920 (2005)
- 12 A. Cotel, A. Jullien, N. Forget, O. Albert, G. Chériaux, C. Le Blanc, *Appl. Phys. B* **83**, 7 (2006)
- 13 N. Minkovski, G.I. Petrov, S.M. Saitiel, O. Albert, J. Etchepare, *J. Opt. Soc. Am. B* **21**, 1659 (2004)
- 14 A. Jullien, O. Albert, G. Chériaux, J. Etchepare, S. Kourtev, N. Minkovski, S.M. Saitiel, *J. Opt. Soc. Am. B* **22**, 2635 (2005)
- 15 N. Minkovski, S.M. Saitiel, G.I. Petrov, O. Albert, J. Etchepare, *Opt. Lett.* **27**, 2025 (2002)
- 16 A. Jullien, O. Albert, G. Chériaux, J. Etchepare, S. Kourtev, N. Minkovski, S.M. Saitiel, *Opt. Express* **14**, 2760 (2006)
- 17 S. Kourtev, N. Minkovski, S.M. Saitiel, A. Jullien, O. Albert, G. Chériaux, J. Etchepare, in *Proc.: LTL Plovdiv’2005, IV Int. Symp. laser technologies and lasers* (Plovdiv, Bulgaria), in print
- 18 O. Albert, J. Etchepare, A. Jullien, G. Chériaux, S. Saitiel, N. Minkovski, *Filtre non linéaire d’impulsions femtosecondes à contraste élevé*, patent: (French, European and US) 11 2004. Publication number: 2 878 657 (int Cl: H 01 S 3/10)